Z. Angew. Math. Phys. (2021) 72:61

0044-2275/21/020001-18
*published online* March 8, 2021
https://doi.org/10.1007/s00033-021-01505-x

**Zeitschrift für angewandte Mathematik und Physik ZAMP**


# Self-similar generalized Riemann problems for the 1-D isothermal Euler system

Helge Kristian Jenssen and Yushuang Luo

**Abstract.** We consider self-similar solutions to the 1-dimensional isothermal Euler system for compressible gas dynamics. For each $\beta \in \mathbb{R}$, the system admits solutions of the form

$$\rho(t,x) = t^{\beta}\Omega(\xi) \qquad u(t,x) = U(\xi) \qquad\qquad \xi = \tfrac{x}{t},$$

where $\rho$ and $u$ denote the density and velocity fields. The ODEs for $\Omega$ and $U$ can be solved implicitly and yield the solution to generalized Riemann problems with initial data

$$\rho(0,x) = \begin{cases} R_l|x|^{\beta} & x<0 \\ R_r x^{\beta} & x>0 \end{cases} \qquad u(0,x) = \begin{cases} U_l & x<0 \\ U_r & x>0, \end{cases}$$

where $R_l$, $R_r > 0$ and $U_l$, $U_r$ are arbitrary constants. For $\beta \in (-1,0)$, the data are locally integrable but unbounded at $x=0$, while for $\beta \in (0,1)$, the data are locally bounded and continuous but with unbounded gradients at $x=0$. Any (finite) degree of smoothness of the data is possible by choosing $\beta > 1$ sufficiently large and $U_l = U_r$. (The case $\beta \le -1$ is unphysical as the initial density is not locally integrable and is not treated in this work.) The case $\beta = 0$ corresponds to standard Riemann problems whose solutions are combinations of backward and forward shocks and rarefaction waves. In contrast, for $\beta \in (-1,\infty) \setminus \{0\}$, we construct the self-similar solution and show that it always contains exactly two shock waves. These are necessarily generated at time 0+ and move apart along straight lines. We provide a physical interpretation of the solution structure and describe the behavior of the solution in the emerging wedge between the shock waves.

**Mathematics Subject Classification.** 35L65, 35L67, 76N10.

**Keywords.** Self-similar solution, Isothermal Euler system, Generalized Riemann problem.

## 1. Introduction and main result

Consider a system of hyperbolic conservation laws in one space dimension,

$$v_t + F(v)_x = 0 \tag{1.1}$$

where $v = v(t,x)$ takes values in an open set $\mathcal{V} \subset \mathbb{R}^n$. A *standard Riemann problem* (SRP) refers to the particular type of initial value problem where the initial data consist of two constant states separated by a jump discontinuity, i.e.,

$$v(0,x) = \begin{cases} v_l & x<0 \\ v_r & x>0, \end{cases}$$

where $v_l$, $v_r \in \mathcal{V}$ are constant vectors. The study of SRPs was initiated by Riemann in the foundational work 'On the propagation of planar air waves of finite amplitude' (see [14]) where the SRP for isentropic Euler flows was resolved. Later progress in fluid flow motivated a general study of such problems, culminating in Lax' resolution of SRPs for general systems (1.1) [9]. In 1965, Glimm [6] showed how SRPs can be used as building blocks in a numerical scheme which provides existence of global-in-time weak

solutions to (1.1) whenever the initial data $v(0,x)$ have sufficiently small variation. For comprehensive treatments, see [4,15].

A *generalized Riemann problem* (GRP) refers to an initial value problem for (1.1) where the data are of the form

$$v(0,x) = \begin{cases} v_l(x) & x < 0 \\ v_r(x) & x > 0, \end{cases}$$

where $v_l$ and $v_r$ now denote given, smooth functions. In this work, we study a special class of GRPs for the isothermal Euler system

$$\rho_t + (\rho u)_x = 0 \tag{1.2}$$

$$(\rho u)_t + (\rho u^2 + a^2\rho)_x = 0, \tag{1.3}$$

where $\rho$ and $u$ are the density and velocity fields, respectively. The pressure field is $p = a^2\rho$, where $a > 0$ is a constant.

The GRPs in question are obtained by insisting that the initial data should generate self-similar solutions of the form

$$\rho(t,x) = t^\beta \Omega(\xi) \qquad u(t,x) = U(\xi) \qquad \xi = \tfrac{x}{t}, \tag{1.4}$$

for a similarity exponent $\beta \in \mathbb{R}$. We shall see that for this to be the case, the initial data must necessarily be of the form

$$\rho(0,x) = \begin{cases} R_l|x|^\beta & x < 0 \\ R_r x^\beta & x > 0 \end{cases} \qquad u(0,x) = \begin{cases} U_l & x < 0 \\ U_r & x > 0, \end{cases} \tag{1.5}$$

where $R_l$, $R_r > 0$ and $U_l$, $U_r$ are constants. See Section 2.

We observe that when $\beta \le -1$ the initial density in (1.5) is not locally integrable at $x = 0$, and the initial data are thus unphysical in this case. It is noteworthy that no self-similar solution appears to solve (1.2)–(1.3) in this case. Throughout, we shall deal exclusively with $\beta$-values strictly larger than $-1$.

Another particular case is $\beta = 0$: (1.5) then prescribes an SRP whose solution consists of constant states connected by one forward and one backward wave, each of which is either a centered rarefaction wave or a shock wave (see [15]). There are thus four different solution structures in the standard case: $\overleftarrow{\mathrm{R}}\overrightarrow{\mathrm{R}}$, $\overleftarrow{\mathrm{R}}\overrightarrow{\mathrm{S}}$, $\overleftarrow{\mathrm{S}}\overrightarrow{\mathrm{R}}$, and $\overleftarrow{\mathrm{S}}\overrightarrow{\mathrm{S}}$.

The main goal of the present work is to show that for all values of $\beta \in (-1,\infty) \setminus \{0\}$ the GRP for (1.2)–(1.3) with data (1.5) necessarily generates exactly two shock waves propagating along straight lines emanating from $x = 0$ at $t = 0$. Thus, the solution structure is in a sense simpler than in the case of SRPs ($\beta = 0$); see Remark 3.1 for a discussion of the technical reason for the difference between the two cases.

Our main result is the following.

**Theorem 1.1.** *For $\beta \in (-1,\infty) \setminus \{0\}$ and for any choice of constants $R_l$, $R_r > 0$ and $U_l$, $U_r \in \mathbb{R}$, the self-similar GRP (1.5) for the 1-dimensional isothermal Euler system (1.2)–(1.3) has a self-similar solution (1.4) of the following form:*

$$\rho(t,x) = \begin{cases} t^\beta \Omega_-\left(\frac{x}{t}\right) & \frac{x}{t} < \bar\xi_- \\ t^\beta \Omega_0\left(\frac{x}{t}\right) & \bar\xi_- < \frac{x}{t} < \bar\xi_+ \\ t^\beta \Omega_+\left(\frac{x}{t}\right) & \frac{x}{t} > \bar\xi_+, \end{cases} \qquad u(t,x) = \begin{cases} U_-\left(\frac{x}{t}\right) & \frac{x}{t} < \bar\xi_- \\ U_0\left(\frac{x}{t}\right) & \bar\xi_- < \frac{x}{t} < \bar\xi_+ \\ U_+\left(\frac{x}{t}\right) & \frac{x}{t} > \bar\xi_+, \end{cases} \tag{1.6}$$

*where the smooth functions $\Omega_{\pm,0}$, $U_{\pm,0}$, and the constants $\bar\xi_\pm$ are determined from the initial data as described in Sects. 4.1–4.2. The solution necessarily contains exactly two entropy admissible (compressive) shocks: a 1-shock moving along $x = \bar\xi_- t$ and a 2-shock moving along $x = \bar\xi_+ t$. The shocks are present for all times $t > 0$.*

The proof of the theorem, while making up most of the present work, requires only elementary considerations based on monotonicity properties of functions that are explicitly available. The argument amounts to showing how the Rankine–Hugoniot conditions for the two shocks select a unique self-similar solution in the central region between them.

We have found it useful to contrast the resolution of GRPs, as described in Theorem 1.1, with the simpler construction of solutions to SRPs (see Sect. 1.1). Before doing so, we include some observations about the result and how it relates to other works in the field.

First, the solutions described by Theorem 1.1 provide non-trivial examples of weak entropy admissible solutions to the isothermal Euler system. Besides their intrinsic interest, they supply relevant test cases for computational codes. Concerning the initial data, we note the following points:

(i) for $\beta \in (-1, 0)$, the initial density is locally integrable but unbounded at $x = 0$;
(ii) for $\beta \in (0, 1)$, the initial density is locally bounded and continuous, but with unbounded gradients as $|x| \downarrow 0$;
(iii) for $\beta > 1$, the initial density is locally bounded and belongs to $C^1(\mathbb{R})$;
(iv) for any integer $k \geq 1$, by choosing $\beta > k$ and $U_l = U_r$, we obtain $C^k(\mathbb{R})$ initial data.

According to (i) and (ii), it is unsurprising that the resulting solution necessarily contains two shock waves when $|\beta| < 1$. Indeed, for $\beta \in (-1, 0)$ the initial density, and hence pressure, contains an unbounded spike at the origin. It is to be expected that such a pressure field will always generate shocks in both characteristic families, no matter what (constant) velocities the fluid has initially on either side of $x = 0$. When $\beta \in (0, 1)$, the infinite pressure gradients on either side of $x = 0$ lead to the same type of behavior: immediate generation of shock waves.

On the other hand, it might appear somewhat surprising that the same solution structure necessarily prevails for $\beta \geq 1$, independently of the initial velocities $U_r$ and $U_l$. For example, it would appear reasonable that a GRP with initial data (1.5) where, say, $R_r = R_l$ and $U_l = -U_r$, with $U_r$ large positive, would generate a smooth flow—at least for an initial time interval. However, Theorem 1.1 asserts that this is not what happens, and instead the flow suffers immediate shock formation also in this case. In fact, as highlighted by (iv) above, our result implies that no (finite) degree of smoothness of the data prevents the presence of shocks at time $t = 0+$.

Of course, this is less surprising once we take into account that whenever $\beta > 0$ the initial density vanishes at the origin, i.e., there is a vacuum state present at $t = 0$. The result in Theorem 1.1 demonstrates that the pressure gradients that *are* present near the initial vacuum at $x = 0$, although small for $\beta$ large, are always sufficiently strong to cause immediate shock formation in the type of self-similar solutions under consideration.

**Remark 1.1.** (Vacuum and shock formation) The Euler system degenerates at $\rho = 0$ and the presence of a vacuum state is analytically challenging. The general problem of obtaining and accurately describing Euler flows with vacuum has received much attention. There are general existence results available for both isentropic (i.e., the pressure is proportional to $\rho^\gamma$ with $\gamma > 1$) and isothermal flows with initially bounded, and possibly vanishing, density field ([5,11,12]). These results, established via vanishing viscosity and compensated compactness, give abstract existence theorems. They do not provide detailed information about the solution near a fluid–vacuum interface. For the latter, see [8].

Closer to the setting of the present work, we note that it is well known how SRPs for isentropic flow yields a self-similar solution with shock and rarefaction waves (see Sect. 1.1). This includes cases with a vacuum on one side as well as cases where the density is strictly positive initially but a vacuum opens up at time $t = 0+$; see [7,15]. In contrast, the latter scenario is not possible for the isothermal model considered in this work: a solution with vacuum-free initial data (of locally bounded variation) remains vacuum-free for all times, [13].

Finally, the issue of finite time singularity formation in 1-D Euler flows has recently received renewed attention. Building on Lax' classic analysis of gradient blowup, the formation of shocks in isentropic flow

with (possibly large) $C^1$ data away from vacuum has been characterized, [1,10]. A key step in [1] is the proof of a lower bound on the density; see also [2,3]. Theorem 1.1 highlights the possibility of *immediate* shock formation (for isothermal flow) in the absence of either upper or lower bounds on the initial density.

### 1.1. Solving SRPs versus GRPs

The proof of Theorem 1.1 is detailed in Sects. 3–5 and requires only elementary arguments. However, it is also somewhat involved and we want to indicate why this is so by contrasting it with the well-known procedure for resolving SRPs.

First, recall the construction of the solution to the SRP $((R_l, U_l), (R_r, U_r))$ for (1.2)–(1.3). The solution is a function of only $\xi = \frac{x}{t}$ (i.e., $\beta = 0$ in (1.4)), and it is assembled from two types of self-similar 'building blocks': constant states and smooth rarefaction solutions. The latter are given by 1-parameter families (one for each characteristic field) of solutions of the ODE system (2.4)–(2.5) with $\beta = 0$; they are explicitly given in (3.14). With these explicit building blocks available, the issue reduces to determining which waves (either a shock or a centered rarefaction) will appear in each characteristic family. As is well known (see [15]), this is conveniently done by first identifying the so-called wave curves in the $(\rho, u)$-plane through, say, the left state $(R_l, U_l)$. These curves partition the $(\rho, u)$-plane into four regions, and the wave structure ($\overleftarrow{\mathrm{R}}\overrightarrow{\mathrm{R}}$, $\overleftarrow{\mathrm{R}}\overrightarrow{\mathrm{S}}$, $\overleftarrow{\mathrm{S}}\overrightarrow{\mathrm{R}}$, or $\overleftarrow{\mathrm{S}}\overrightarrow{\mathrm{S}}$) of the solution is determined by identifying which region contains the right state $(R_r, U_r)$.

Turning to GRPs with initial data (1.5), the situation is different. For SRPs, the wave curves mentioned above connect those pairs of *constant states* that can be joined by a single shock or rarefaction. For GRPs, the 'states' to be connected are not constant states but instead dynamically changing solutions of the form (1.4). This is the main reason why resolving GRPs is more involved than resolving SRPs. It requires a detailed study of the similarity ODEs satisfied by the functions $\Omega_{\pm,0}$ and $U_{\pm,0}$ appearing in Theorem 1.1.

A simplifying feature of the isothermal Euler system is that the ODE for $U(\xi)$ decouples and can be solved in isolation and yields an implicit relation between $\xi$ and $U$; see (3.3)–(3.4). (This is essentially a consequence of the fact that the density appears *linearly* in (1.2)–(1.3).) In turn, this gives the corresponding $\Omega(\xi)$-values in terms of $U(\xi)$; see (3.6)–(3.7).

From the initial data (1.5), we first need to identify the solution in the regions on the far right and far left in the $(x, t)$-plane, i.e., for $|\xi| \gg 1$. (In contrast, for SRPs these parts of the solution are simply the constant states given by the initial data.) These 'extreme' solutions, denoted $(\Omega_\pm, U_\pm)$ in Theorem 1.1, are implicitly given in terms of the initial data via (4.2)–(4.4) and (4.7). Having determined the far left and far right parts of the solution, it remains to connect them to the, as yet unknown, 'intermediate' solution $(U_0, \Omega_0)$ via admissible shocks. It is part of the problem to determine the locations of these shocks.

We show below how the Rankine–Hugoniot relations for the two shocks yield four nonlinear equations for four unknown constants $\bar{C}$, $\bar{K}$, and $\bar{\xi}_\pm$. The first two specify the intermediate solution $(U_0, \Omega_0)$, while $\bar{\xi}_\pm$ give the paths of the emerging shock waves. An argument based on monotonicity shows that the four equations possess a unique solution. We have found it convenient to organize the analysis so that one first identifies $\bar{C}$ from an explicitly given equation (see (4.28)), which in turn yields $\bar{K}$ (Lemma 4.2). Finally, $\bar{\xi}_\pm$ are determined as the unique roots of two explicitly available equations (see (4.15)–(4.16) and Lemma 4.1).

### 1.2. Plan of the paper

The rest of the work is organized as follows. Section 2 reviews briefly the form of self-similar solutions to the isothermal Euler model, describes their initial data, and derives the associated similarity ODEs. In

Sect. 3, we record certain symmetry properties of these ODEs and derive their solutions (in implicit form). We introduce two types of reference solutions, and record their properties, which differ for $\beta \in (-1,0)$ and $\beta \in (0,\infty)$. Section 3 also includes a brief outline of how these solutions are used to resolve GRPs of the form (1.5) for (1.2)–(1.3). The, somewhat lengthy, details for the case $\beta \in (-1,0)$ are given in Section 4. The argument for the case $\beta \in (0,\infty)$ is almost identical and is outlined in Sect. 5, concluding the proof of Theorem 1.1. Finally, Sect. 6 provides some additional qualitative (and $\beta$-dependent) properties of the solutions in the region between the two shock waves.

## 2. Self-similar solutions

### 2.1. Self-similar GRPs and similarity ODEs

Let $(\rho, u)$ be a solution of (1.2)–(1.3) with initial data

$$\rho(0,x) = \rho_0(x) \qquad u(0,x) = u_0(x).$$

For $\lambda \in \mathbb{R}_+$, set

$$\rho_\lambda(t,x) := \lambda^A \rho(\lambda^B t, \lambda^C x) \qquad u_\lambda(t,x) := \lambda^D u(\lambda^B t, \lambda^C x).$$

A direct calculation shows that $(\rho_\lambda, u_\lambda)$ is again a solution of (1.2)–(1.3) provided $C = B$ and $D = 0$. *Self-similarity* of the given solution requires further that $(\rho_\lambda, u_\lambda) \equiv (\rho, u)$ for all $\lambda \in \mathbb{R}_+$, i.e.,

$$\lambda^A \rho(\lambda^B t, \lambda^B x) = \rho(t,x) \qquad u(\lambda^B t, \lambda^B x) = u(t,x) \tag{2.1}$$

for all $\lambda \in \mathbb{R}_+$, and for all $(t,x) \in \mathbb{R}_+ \times \mathbb{R}$. Choosing $\lambda = t^{-\frac{1}{B}}$ and setting $\beta := -\frac{A}{B}$ show that a self-similar solution of the isothermal Euler system must have the form

$$\rho(t,x) = t^\beta \Omega(\xi) \qquad u(t,x) = U(\xi), \qquad \xi = \frac{x}{t}. \tag{2.2}$$

On the other hand, evaluating (2.1) at time $t = 0$ yields

$$\lambda^A \rho_0(\lambda^B x) = \rho_0(x) \quad \text{and} \quad u_0(\lambda^B x) = u_0(x) \quad \text{for all } \lambda \in \mathbb{R}_+ \text{ and all } x \in \mathbb{R}.$$

Applying this with $\lambda = |x|^{-\frac{1}{B}}$ shows that $|x|^\beta \rho_0(\mathrm{sgn}(x)) = \rho_0(x)$ and $u_0(\mathrm{sgn}(x)) = u_0(x)$ for all $x \in \mathbb{R}$. This shows that the initial data of a self-similar solution must have the form

$$\rho(0,x) = \begin{cases} R_l |x|^\beta & x < 0 \\ R_r x^\beta & x > 0 \end{cases} \qquad u(0,x) = \begin{cases} U_l & x < 0 \\ U_r & x > 0, \end{cases} \tag{2.3}$$

where $R_l$, $R_r > 0$ and $U_l$, $U_r$ are arbitrary constants (cf. (1.5)). The similarity exponent $\beta$ is free at this stage.

In the following, we refer to GRPs with initial data of the form (2.3) as *self-similar GRPs*. It requires further analysis to identify the corresponding solutions to (1.2)–(1.3). We do this in Sect. 3, and then use the result to resolve any self-similar GRPs when $\beta \in (-1,\infty) \setminus \{0\}$ in Sects. 4 and 5.

Before doing so, we derive the ODEs that describe self-similar solutions, and also review the jump relations and entropy conditions for discontinuous flows. First, using (2.2) in (1.2)–(1.3) shows that the similarity variables $\Omega$ and $U$ satisfy the ODEs

$$(U - \xi)\frac{\Omega'}{\Omega} + U' + \beta = 0 \tag{2.4}$$

$$a^2 \frac{\Omega'}{\Omega} + (U - \xi)U' = 0, \tag{2.5}$$

where $' \equiv \frac{d}{d\xi}$. A simplifying feature of the isothermal case is that $U$ satisfies a single, decoupled ODE: solving for $U'$ and $\frac{\Omega'}{\Omega}$ yields

$$U' = \frac{\beta a^2}{(U-\xi)^2 - a^2} \tag{2.6}$$

$$\frac{\Omega'}{\Omega} = -\frac{\beta(U-\xi)}{(U-\xi)^2 - a^2}. \tag{2.7}$$

We refer to these equations as the *similarity ODEs*. The latter system is equivalent to (2.4)–(2.5) provided the determinant $(U-\xi)^2 - a^2$ does not vanish. We shall verify below that this is indeed the case for the solutions we consider in this work. In fact, it is immediate to verify that $U(\xi) = \xi \pm a$, together with $\Omega(\xi) = const. \exp(\mp\frac{\xi}{a})$, provide solutions to (2.4)–(2.5) if and only if $\beta = 0$. This is the case of an SRP, which is not part of the following analysis. See Remark 3.1 for a comparison of GRPs and SRPs.

### 2.2. Characteristics; jump relations; similarity shocks

In isothermal flow (1.2)–(1.3), the sound speed is constant equal to $a$, and the characteristic speeds are

$$\lambda_1 = u - a \qquad \lambda_2 = u + a. \tag{2.8}$$

If the solution suffers a jump discontinuity across the curve $x = x(t)$, the Rankine–Hugoniot relations take the form

$$\dot{x}\llbracket\rho\rrbracket = \llbracket\rho u\rrbracket \qquad \dot{x}\llbracket\rho u\rrbracket = \llbracket\rho(u^2 + a^2)\rrbracket. \tag{2.9}$$

Here and below, we use the convention that for any flow quantity $q$,

$$\llbracket q\rrbracket := q^+ - q^- \equiv q(t, x(t)+) - q(t, x(t)-).$$

The Lax entropy condition for 1- and 2-shocks requires

$$\lambda_1^- > \dot{x} > \lambda_1^+, \qquad \text{i.e.,} \qquad u^- > \dot{x} + a > u^+, \tag{2.10}$$

and

$$\lambda_2^- > \dot{x} > \lambda_2^+, \qquad \text{i.e.,} \qquad u^- > \dot{x} - a > u^+, \tag{2.11}$$

respectively. A calculation shows that these conditions amount to compressivity of the shocks: a parcel of fluid passing through a shock suffers an increase in density (see [15]).

Next consider a 'similarity shock' in 1-d isothermal flow: the shock is assumed to propagate along a path of the form $\xi \equiv \bar{\xi}$, i.e., $x(t) = \bar{\xi}t$. It is assumed that the density and velocity on each side of the shock are of the form (2.2), with $\beta$ taking the same value on both sides. Letting $(U^+, \Omega^+)$ and $(U^-, \Omega^-)$ denote the parts of the solution on the right and left of the shock, respectively, the Rankine–Hugoniot relations (2.9) reduce to

$$\bar{\xi}\llbracket\Omega\rrbracket = \llbracket\Omega U\rrbracket \qquad \bar{\xi}\llbracket\Omega U\rrbracket = \llbracket\Omega(U^2 + a^2)\rrbracket, \tag{2.12}$$

where $\llbracket\cdot\rrbracket$ now denotes jump across $\xi = \bar{\xi}$. The Lax entropy conditions (2.10)–(2.11) take the form

$$U^-(\bar{\xi}) > \bar{\xi} + a > U^+(\bar{\xi}) \qquad \text{for a 1-shock} \tag{2.13}$$

$$U^-(\bar{\xi}) > \bar{\xi} - a > U^+(\bar{\xi}) \qquad \text{for a 2-shock.} \tag{2.14}$$

Setting $V^\pm := \bar{\xi} - U^\pm$, where $U^\pm = U^\pm(\bar{\xi})$, the Rankine–Hugoniot conditions take the form

$$\llbracket\Omega V\rrbracket = 0 \tag{2.15}$$

$$\llbracket\Omega(V^2 + a^2)\rrbracket = 0. \tag{2.16}$$

It follows from these that

$$V^+V^- = a^2, \tag{2.17}$$

and that an equivalent form of the jump conditions is given by

$$U^+ - \bar{\xi} = \frac{a^2}{U^- - \bar{\xi}} \qquad \text{and} \qquad \Omega^+ = \frac{(U^- - \bar{\xi})^2}{a^2}\Omega^-. \tag{2.18}$$

Equivalently, solving for $V^-$ and $\Omega^-$, we have

$$U^- - \bar{\xi} = \frac{a^2}{U^+ - \bar{\xi}} \qquad \text{and} \qquad \Omega^- = \frac{(U^+ - \bar{\xi})^2}{a^2}\Omega^+. \tag{2.19}$$

## 3. Integration of similarity ODEs

We proceed to solve the ODE system (2.6)–(2.7), and focus first on the decoupled ODE for $U(\xi)$. We start with two observations that effectively reduce the general case to one of two particular cases.

**Lemma 3.1.** *Assume that $U(\xi)$ is a solution of (2.6); then so are the functions $\xi \mapsto C + U(\xi - C)$ for any constant $C$, as well as the function $\xi \mapsto -U(-\xi)$.*

*Proof.* Direct calculation. □

This shows that a 45° translate in the $(\xi, U)$-plane of the graph of a solution to (2.6) yields the graph of another solution; ditto for its reflection about the origin.

In the following, we restrict attention to $\beta$-values in the set $(-1, \infty)\setminus\{0\}$; see Remark 3.1. To integrate (2.6), we first interchange the roles of the dependent and independent variables and introduce the new unknown $V(U) := \xi(U) - U$ to obtain the ODE

$$V'(U) = \frac{1}{\beta a^2}(V^2 - \mu^2), \tag{3.1}$$

where we have set

$$\mu := a\sqrt{1+\beta} > 0. \tag{3.2}$$

The two trivial solutions $V(U) \equiv \pm\mu$ of (3.1) yield two special, straight line solutions $U(\xi) = \xi \pm \mu$ of (2.6). It turns out that the latter solutions are irrelevant for the resolution of the self-similar GRPs under consideration in this work. Their only role is that of providing the asymptotic behavior of solutions that are relevant for resolving self-similar GRPs. (See Figs. 1 and 2.)

All other solutions of (3.1), and thus of (2.6), are obtained by direct integration, giving $\xi$ as a function of $U$. These solutions are of one of two types:

$$\text{Type I:} \qquad \xi = U - \mu\coth[\alpha(U - C)], \tag{3.3}$$

and

$$\text{Type II:} \qquad \xi = U - \mu\tanh[\alpha(U - C)], \tag{3.4}$$

where $C$ is an arbitrary constant of integration and

$$\alpha := \frac{\mu}{\beta a^2} = \frac{\sqrt{1+\beta}}{a\beta}. \tag{3.5}$$

With $\xi - U$ expressed in terms of $U$ by (3.3)–(3.4), it is immediate to integrate (2.5) and obtain $\Omega$ in terms of $U$. For each type of $U$-solution given by (3.3) and (3.4), we obtain the corresponding $\Omega$-solutions:

$$\text{Type I:} \qquad \Omega(\xi) = K|\sinh[\alpha(U(\xi) - C)]|^{-\beta}, \tag{3.6}$$

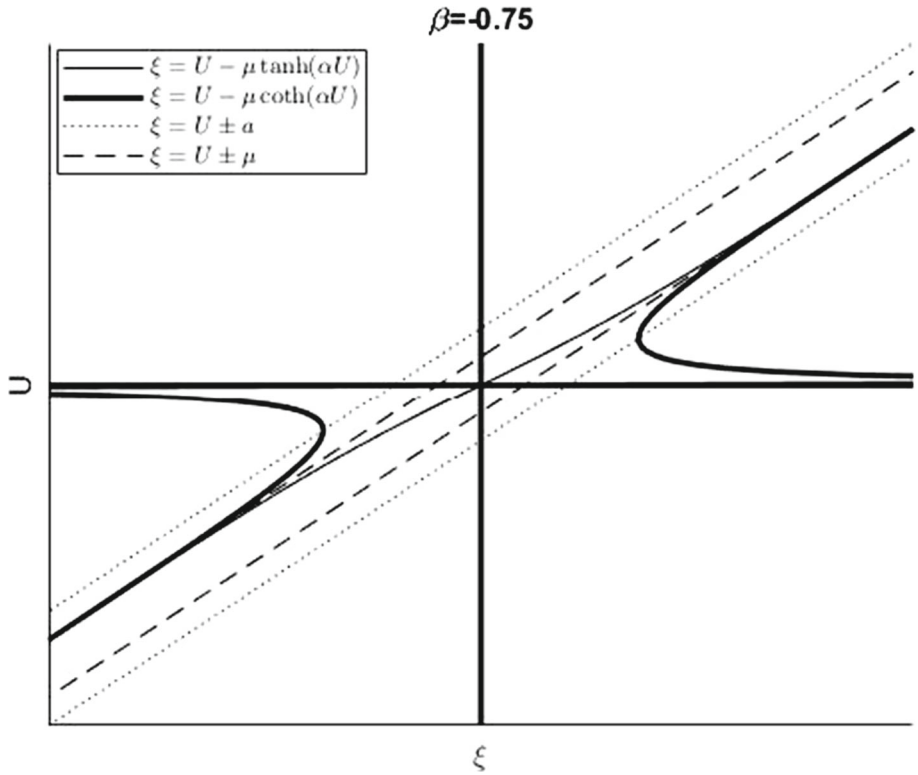


FIG. 1. Type I (thick solid line) and Type II (thin solid line) reference solutions when $\beta = -0.75$

and

$$\text{Type II:} \qquad \Omega(\xi) = K(\cosh[\alpha(U(\xi) - C)])^{-\beta}, \tag{3.7}$$

where $K > 0$ denotes an arbitrary constant of integration, and $C$ is as in (3.3) and (3.4), respectively.

Returning to the velocity field, we introduce the '45°-strip'

$$\mathcal{S}_\mu := \{(\xi, U) \,:\, |U - \xi| < \mu\}$$

in the $(\xi, U)$-plane. It follows from Lemma 3.1 that:

- the graphs of all Type I solutions are located outside of $\mathcal{S}_\mu$ and are 45° translates of the graphs of the solutions $U(\xi)$ of (2.6) given implicitly by

$$\xi = U(\xi) - \mu \coth[\alpha U(\xi)]; \tag{3.8}$$

- the graphs of all Type II solutions are located within $\mathcal{S}_\mu$ and are 45° translates of the graphs of the solutions $U(\xi)$ of (2.6) given implicitly by

$$\xi = U(\xi) - \mu \tanh[\alpha U(\xi)]. \tag{3.9}$$

### 3.1. Reference solutions for $\beta \in (-1, 0)$

Figure 1 shows the Type I and Type II solutions given by (3.8) and (3.9) in a representative case for $\beta \in (-1, 0)$. In fact, as illustrated by the graphs in Fig. 1, (3.8) yields four distinct branches of solutions

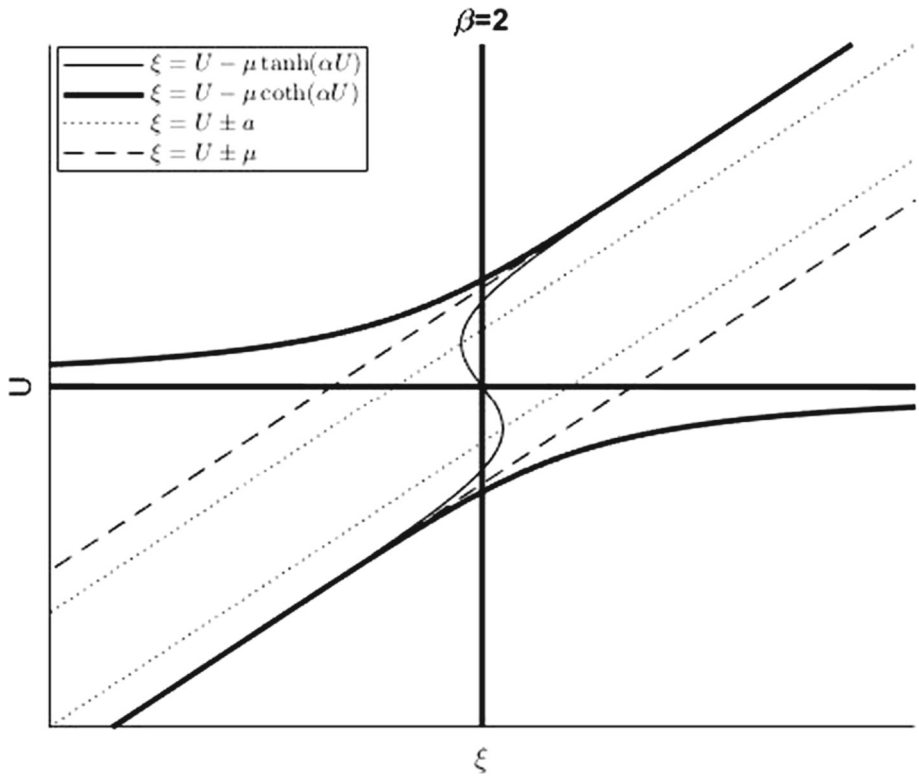


FIG. 2. Type I (thick solid line) and Type II (thin solid line) reference solutions when $\beta = 2$

$U(\xi)$. Two of these have $U(\xi)$ positive and are defined for $\xi \geq \xi^*$, where $\xi^*$ is given implicitly by

$$\tanh[|\alpha|(\xi^* - a)] = \sqrt{1+\beta}. \tag{3.10}$$

The other two (negative-valued) branches are obtained from the former ones by reflection about the origin in the $(\xi, U)$-plane.

The two positive branches meet at the point $(\xi^*, \xi^* - a)$, where they both have infinite slope. In solving self-similar GRPs, we shall only need the lower of these two branches, which we from now on refer to as the *Type I reference solution for* $\beta \in (-1, 0)$ and denote by $\hat{U}(\xi)$. We note that $\hat{U}(\xi)$ is strictly decreasing on $[\xi^*, \infty)$ and tends to zero as $\xi \uparrow \infty$; its graph is located below the straight line $U = \xi - a$. For later reference, we note that $U^* := \hat{U}(\xi^*) = \xi^* - a$ is given implicitly by

$$\tanh[|\alpha|U^*] = \sqrt{1+\beta}. \tag{3.11}$$

As illustrated in Fig. 1, for $\beta \in (-1, 0)$, (3.9) yields a single, strictly increasing solution; we refer to it as the *Type II reference solution for* $\beta \in (-1, 0)$ and denote it by $\bar{U}(\xi)$. We note that its graph is located within the 45°-strip $\{(\xi, U) : |U - \xi| < \mu\}$.

### 3.2. Reference solutions for $\beta \in (0, \infty)$

Figure 2 shows the Type I and Type II solutions in a representative case for $\beta \in (0, \infty)$. The situation in this case is as follows. There are now two solutions $U(\xi)$ to (3.8) whose graphs are located outside the 45°-strip $\{(\xi, U) : |U - \xi| < \mu\}$; they are both defined for all $\xi \in \mathbb{R}$, and are reflections of each other

through the origin. The one whose graph is located below the straight line $U = \xi - \mu$ is referred to as the *Type I reference solution for* $\beta \in (0, \infty)$ and again denoted by $\hat{U}(\xi)$.

Finally, as illustrated in Fig. 2, for $\beta \in (0, \infty)$, (3.9) yields an 'S'-shaped curve located within the 45°-strip $\{(\xi, U) : |U - \xi| < \mu\}$. This curve defines three solution branches. Two are located within the 45°-strips $\{(\xi, U) : a < |U - \xi| < \mu\}$. The subsequent analysis outlined in Sect. 5 shows that these curves are not used in the solution of self-similar GRPs. The remaining branch, which will be of use, defines a strictly decreasing solution to (3.9). We refer to it as the *Type II reference solution for* $\beta \in (0, \infty)$ and again denote it by $\bar{U}(\xi)$. We note that its graph is located within the 45°-strip $\{(\xi, U) : |U - \xi| \leq a\}$ and that $\bar{U}(\xi)$ is defined for $\xi \in (-\xi^*, \xi^*)$, where $\xi^* > 0$ is now implicitly given by

$$\tanh[\alpha(a - \xi^*)] = \tfrac{1}{\sqrt{1+\beta}}. \tag{3.12}$$

It follows that, for $\beta \in (0, \infty)$, the value $U^* := \bar{U}(-\xi^*) = a - \xi^*$ is given implicitly by

$$\tanh[\alpha U^*] = \tfrac{1}{\sqrt{1+\beta}}. \tag{3.13}$$

**Remark 3.1.** As noted earlier, the situation is different in the case of SRPs, i.e., when $\beta = 0$. In that case

$$(U(\xi), \Omega(\xi)) = (\xi \pm a, C \exp(\mp \tfrac{\xi}{a})) \qquad (C \in \mathbb{R}) \tag{3.14}$$

are solutions of (2.4)–(2.5), and together with constant vectors they provide all self-similar solutions $(\rho(t, x), u(t, x)) = (\Omega(\frac{x}{t}), U(\frac{x}{t}))$ of the isothermal Euler system in this case.

This points out a key difference between SRPs and self-similar GRPs. As is evident from the preceding analysis, the graphs of the Type I and Type II solutions $\hat{U}(\xi)$ and $\bar{U}(\xi)$ for $\beta \in (-1, \infty) \setminus \{0\}$ never intersect the special straight line solutions $U = \xi \pm \mu$. In contrast, for $\beta = 0$ the special straight line solutions are $U = \xi \pm a$, and these intersect any constant $U$-solution.

The upshot is that in the latter case it is possible to continuously connect any constant solution to one of the special, straight line solutions. This corresponds to the presence of weak discontinuities (gradient discontinuities), and this is how centered rarefaction waves connect to constant states in the resolution of SRPs. This feature is absent in self-similar GRPs with $\beta \neq 0$, which explains why the solutions described in Theorem 1.1 contain shocks and no weak discontinuities.

### 3.3. Resolving self-similar GRPs: outline

The Type I and Type II reference solutions defined above, together with their 45°-translates and reflections about the origin in the $(\xi, U)$-plane, will provide the building blocks required to resolve any self-similar GRP.

Before giving the details in Sects. 4 and 5, we give an outline of the solution procedure. For concreteness, consider a $\beta$-value in $(-1, 0)$. Recalling the derivations in Sect. 2.1, we pose the self-similar GRP data (1.5) for the isothermal Euler system (1.2)–(1.3). The first step is to observe that if $x > 0$, say, then $\xi = \frac{x}{t} \uparrow \infty$ as $t \downarrow 0$. Therefore, the solution $U(\xi)$ of (2.6) to be used for 'large,' positive $\xi$-values must satisfy

$$\lim_{\xi \uparrow \infty} U(\xi) = U_r.$$

It follows from the analysis above that this requirement singles out a unique solution $U_+(\xi)$ of (2.6): its graph must necessarily be (a part of) a certain 45°-translate of the graph of the Type I reference solution in this case. (This follows because the latter solutions are the only type of solutions with a finite limit at $\xi = \infty$ in this case.) Specifically, $U_+(\xi)$ must satisfy (3.3) with $C = U_r$.

An entirely similar argument selects a unique solution $U_-(\xi)$ to be used for large, negative values of $\xi$, and which must satisfy

$$\lim_{\xi\downarrow-\infty} U_-(\xi) = U_l.$$

Its graph is obtained from that of the Type I reference solution in this case by a 45°-translation followed by reflection about the origin. In particular, $U_-(\xi)$ must satisfy (3.3) with $C = U_l$. With this, we have used the initial $U$-values in (1.5) to determine what the self-similar velocity field must be for large values of $|\xi| = \frac{|x|}{t}$.

The next step is to determine the velocity field for intermediate $\xi$-values, and we shall see that this can always be accomplished (in a unique manner) by inserting two shock waves that connect the solutions $U_\pm(\xi)$ determined above to a certain translate of the Type II reference solution. For this, the issue is to identify unique jump locations $\bar\xi_\pm$ (with $\bar\xi_- < \bar\xi_+$), together with a unique 45°-translate $U_0(\xi) = \bar C + \bar U(\xi - \bar C)$ of the Type II reference solution $\bar U$ (which satisfies (3.9)), so that the following criteria are met:

(∗) $U_-(\xi)$ and $U_+(\xi)$ are defined for $\xi < \bar\xi_-$ and $\xi > \bar\xi_+$, respectively;
(∗∗) the discontinuity between $U_-$ and $U_0$ at $\bar\xi_-$, and between $U_0$ and $U_+$ at $\bar\xi_+$, both satisfy the Rankine–Hugoniot relations (2.12).

We note that once these criteria are met, then the Lax entropy conditions in (2.13)–(2.14) are automatically satisfied. This follows because the graphs of $U_-(\xi)$, $U_+(\xi)$, and $U_0(\xi)$ are, by construction, located above, below, and within the 45°-strip $\{(\xi, U) : |U - \xi| \le a\}$, respectively. The Lax conditions (2.13)–(2.14) follow from this: the jump from $U_+(\bar\xi_+)$ to $U_0(\bar\xi_+)$ satisfies the entropy condition for a 2-shock, while the jump from $U_-(\bar\xi_-)$ to $U_0(\bar\xi_-)$ satisfies the entropy condition for a 1-shock.

It remains to describe the density field of the solution, which has the form in $(1.4)_1$. Let $\Omega_\pm$ and $\Omega_0$ denote the solutions of (2.7) corresponding to $U_\pm$ and $U_0$; according to the analysis above, their functional forms are given by (3.6) and (3.7). These $\Omega$-solutions are therefore determined once their multiplicative constants $K_\pm$ and $\bar K$ are found. In Sect. 4.1, we detail how the initial data (specifically, the constants $R_l$ and $R_r$) determine the $K$-values $K_\pm$ for the two Type I solutions which is used for large values of $|\xi|$. The remaining $K$-value $\bar K$ for the Type II solution to be used in the intermediate range $\xi \in (\bar\xi_-, \bar\xi_+)$ must be determined together with the parameters $\bar\xi_\pm$ and $\bar C$. The details of this argument are given in Sect. 4.2.

Summing up: to identify the solution of the self-similar GRP (1.5) with $\beta \in (-1, 0)$ for (1.2)–(1.3), we need to identify the four parameters $\bar\xi_\pm$, $\bar C$, and $\bar K$. It will follow from the analysis in Sect. 4.2 that there is a unique choice of these parameters which provides a solution to the self-similar GRP under consideration. Finally, a similar procedure provides the solution of self-similar GRPs with $\beta \in (0, \infty)$, see Sect. 5.

## 4. Self-similar GRPs for $\beta \in (-1, 0)$

Throughout this section, the similarity exponent $\beta \in (-1, 0)$ is fixed, and we consider the GRP for (1.2)–(1.3) with the initial data in (1.5).

### 4.1. The solution for large values of $|\xi|$

As explained in the previous section, the initial velocities $U_r$ and $U_l$ determine the unique Type I solutions that result for large values of $|\xi| = \frac{x}{t}$. Namely, the resulting velocity field for large positive values of $\xi$ must be $u(t, x) = U_+(\frac{x}{t})$ where $U_+$ satisfies (3.3) with $C = U_r$:

$$\xi = U_+(\xi) - \mu \coth[\alpha(U_+(\xi) - U_r)] \qquad \text{for } \xi \text{ large positive.} \tag{4.1}$$

Similarly, the resulting velocity field for large negative values of $\xi$ must be $u(t,x) = U_-(\frac{x}{t})$ where $U_-$ satisfies (3.3) with $C = U_l$:

$$\xi = U_-(\xi) - \mu \coth[\alpha(U_-(\xi) - U_l)] \qquad \text{for } \xi \text{ large negative.} \tag{4.2}$$

Next, the $\Omega$-solutions $\Omega_\pm(\xi)$ corresponding to $U_\pm(\xi)$ are of the form (3.6):

$$\Omega_+(\xi) = K_+ |\sinh[\alpha(U_+(\xi) - U_r)]|^{-\beta} \qquad \text{for } \xi \text{ large positive,} \tag{4.3}$$

and

$$\Omega_-(\xi) = K_- |\sinh[\alpha(U_-(\xi) - U_l)]|^{-\beta} \qquad \text{for } \xi \text{ large negative.} \tag{4.4}$$

where the multiplicative constants $K_\pm$ must be determined from the coefficients $R_r$ and $R_l$ in the initial data (1.5). To do so, we use the identity $|\sinh s| = (\coth^2 s - 1)^{-\frac{1}{2}}$, together with the expressions in (4.2) and (4.2), to rewrite (4.4) and (4.4) as

$$\Omega_+(\xi) = \frac{K_+}{\mu^\beta}[(\xi - U_+(\xi))^2 - \mu^2]^{\frac{\beta}{2}} \qquad \text{for } \xi \text{ large positive,} \tag{4.5}$$

and

$$\Omega_-(\xi) = \frac{K_-}{\mu^\beta}[(\xi - U_-(\xi))^2 - \mu^2]^{\frac{\beta}{2}} \qquad \text{for } \xi \text{ large negative,} \tag{4.6}$$

respectively. Consider the resulting density field $\rho(t,x)$ for $x > 0$, say, and small times $t$, which according to (4.6) is given by

$$\rho(t,x) = t^\beta \Omega_+(\tfrac{x}{t}) = \frac{K_+}{\mu^\beta}[(x - tU_+(\tfrac{x}{t}))^2 - \mu^2 t^2]^{\frac{\beta}{2}}.$$

Since $U_+(\xi)$ by construction tends to the finite limit $U_r$ as $\xi \uparrow \infty$, we deduce that

$$\lim_{t \downarrow 0} \rho(t,x) = \frac{K_+}{\mu^\beta} x^\beta \qquad \text{for } x > 0,$$

confirming the derivation in Sect. 2.1. A similar conclusion holds when $x < 0$. Comparing with the prescribed initial data (1.5), it follows that the integration constants $K_\pm$ appearing in (4.4) and (4.4) are given by

$$K_+ = \mu^\beta R_r \qquad \text{and} \qquad K_- = \mu^\beta R_l. \tag{4.7}$$

With this, the solution $(\rho(t,x), u(t,x))$ of (1.2)–(1.3) with data (1.5) has been determined for large values of $\frac{|x|}{t}$.

### 4.2. The solution for intermediate values of $|\xi|$; resolution of GRPs

As outlined above, the initial data (1.5) determine the resulting solutions $(U_\pm(\xi), \Omega_\pm(\xi))$ of (2.6)–(2.7), which in turn provide the solution of the self-similar GRP (1.2)–(1.3)–(1.5) for large values of $|\xi| = \frac{|x|}{t}$.

To complete the solution, we shall show that there is a unique Type II solution $(U_0(\xi), \Omega_0(\xi))$ with the property that it connects to the far left solution $(U_-(\xi), \Omega_-(\xi))$ through an admissible 1-shock at some $\xi = \bar{\xi}_-$, and to the far right solution $(U_+(\xi), \Omega_+(\xi))$ through an admissible 2-shock at some $\xi = \bar{\xi}_+ > \bar{\xi}_-$. As noted in Sect. 3.3, these requirements amount to the validity of the Rankine–Hugoniot relations (2.19) at $\bar{\xi}_\pm$. (In particular, the Lax entropy conditions will be automatically satisfied due to the properties of the solutions under consideration.)

Letting $\bar{C}$ and $\bar{K}$ denote the constants of integration determining the Type II solution $(U_0(\xi), \Omega_0(\xi))$ to be used for $\xi \in (\bar{\xi}_-, \bar{\xi}_+)$, we have from (3.4) and (3.7) that

$$\xi = U_0(\xi) - \mu \tanh[\alpha(U_0(\xi) - \bar{C})] \tag{4.8}$$

$$\Omega_0(\xi) = \bar{K}(\cosh[\alpha(U_0(\xi) - \bar{C})])^{-\beta}. \tag{4.9}$$

The goal is to show that there is a unique choice of parameters $\bar{C}$, $\bar{K}$, and $\bar{\xi}_\pm$ so that the criteria $(*)$ and $(**)$ in Sect. 3.3 are both met.

We proceed to write out the Rankine–Hugoniot relations at $\bar{\xi}_\pm$. This will give four equations relating the four parameters $\bar{C}$, $\bar{K}$, $\bar{\xi}_\pm$. We then demonstrate that these equations have a unique solution. At $\bar{\xi}_+$, we substitute from (4.2), (4.4), (4.8), and (4.9) into the Rankine–Hugoniot relations (2.19) to obtain the relations

$$\tanh[\alpha(U_+(\bar{\xi}_+) - U_r)] = (1+\beta)\tanh[\alpha(U_0(\bar{\xi}_+) - \bar{C})] \tag{4.10}$$

and

$$\begin{aligned}&\bar{K}(\cosh[\alpha(U_0(\bar{\xi}_+) - \bar{C})])^{-\beta}\\ &\quad = (1+\beta)K_+|\sinh[\alpha(U_+(\bar{\xi}_+) - U_r)]|^{-\beta}\coth^2[\alpha(U_+(\bar{\xi}_+) - U_r)],\end{aligned} \tag{4.11}$$

where we have also used (3.2).

Similarly, at $\bar{\xi}_-$ we substitute from (4.2), (4.4), (4.8), and (4.9) into the Rankine–Hugoniot relations (2.19) to obtain the relations

$$\tanh[\alpha(U_-(\bar{\xi}_-) - U_l)] = (1+\beta)\tanh[\alpha(U_0(\bar{\xi}_-) - \bar{C})] \tag{4.12}$$

and

$$\begin{aligned}&\bar{K}(\cosh[\alpha(U_0(\bar{\xi}_-) - \bar{C})])^{-\beta}\\ &\quad = (1+\beta)K_-|\sinh[\alpha(U_-(\bar{\xi}_-) - U_l)]|^{-\beta}\coth^2[\alpha(U_-(\bar{\xi}_-) - U_l)].\end{aligned} \tag{4.13}$$

(In the formulae above, $K_\pm$ are given by (4.7).) To analyze the four equations (4.10)–(4.13), it is convenient to express the various Type I and Type II solutions in terms of the Type I reference solution $\hat{U}$ and the Type II reference solution $\bar{U}$ that were introduced in Sect. 3.1. For convenience, we also let

$$\check{U}(\xi) := -\hat{U}(-\xi) \tag{4.14}$$

denote the reflection of $\hat{U}$ about the origin. We then have

$$U_+(\xi) - U_r = \hat{U}(\xi - U_r), \qquad U_-(\xi) - U_l = \check{U}(\xi - U_l), \qquad U_0(\xi) - \bar{C} = \bar{U}(\xi - \bar{C}).$$

With these, we have that (4.10) and (4.12) take the forms

$$\tanh[|\alpha|\hat{U}(\bar{\xi}_+ - U_r)] = (1+\beta)\tanh[|\alpha|\bar{U}(\bar{\xi}_+ - \bar{C})], \tag{4.15}$$

and

$$\tanh[|\alpha|\check{U}(\bar{\xi}_- - U_l)] = (1+\beta)\tanh[|\alpha|\bar{U}(\bar{\xi}_- - \bar{C})], \tag{4.16}$$

respectively (recall that $\alpha < 0$ for $\beta \in (-1, 0)$, cf. (3.5)). Note that $\bar{K}$ does not appear in these two last equations.

The strategy is now to first argue that (4.15) and (4.16) define $\bar{\xi}_\pm$ as functions of $\bar{C}$ (see Lemma 4.1). We shall then show that the Rankine–Hugoniot relation (4.11) yields $\bar{K}$ as a function $\bar{K}_+(\bar{C})$ of $\bar{C}$, and similarly that (4.13) yields $\bar{K}$ as a function $\bar{K}_-(\bar{C})$ of $\bar{C}$. The argument is completed once we verify that there is a unique value of $\bar{C}$ for which $\bar{K}_+(\bar{C}) = \bar{K}_-(\bar{C})$; see Lemma 4.2.

**Lemma 4.1.** *For any choice of $\bar{C} \in \mathbb{R}$, each of Eqs. (4.15) and (4.16) has unique solutions $\bar{\xi}_+ = \bar{\xi}_+(\bar{C})$ and $\bar{\xi}_- = \bar{\xi}_-(\bar{C})$, respectively. Furthermore, both of $\bar{\xi}_\pm(\bar{C})$ are increasing functions of $\bar{C}$ and satisfy*

$$\bar{\xi}_-(\bar{C}) < \bar{C} < \bar{\xi}_+(\bar{C}).$$

*Proof.* Introducing the functions

$$f_+(\xi; U_r) := \tanh[|\alpha|\hat{U}(\xi - U_r)], \qquad f_-(\xi; U_l) := \tanh[|\alpha|\check{U}(\xi - U_l)],$$

and

$$\bar{f}(\xi; \bar{C}) := (1+\beta)\tanh[|\alpha|\bar{U}(\xi - \bar{C})],$$

Eqs. (4.15) and (4.16) take the forms

$$\bar{f}(\xi;\bar{C}) = f_+(\xi;U_r) \qquad \text{and} \qquad \bar{f}(\xi;\bar{C}) = f_-(\xi;U_l), \tag{4.17}$$

respectively. We have that both of $f_\pm$ are strictly decreasing functions of $\xi$, while $\bar{f}$ is a strictly increasing function of $\xi$. More precisely, with

$$\xi_{\min} := U_r + \xi^* \qquad \text{and} \qquad \xi_{\max} := U_l - \xi^*,$$

where $\xi^*$ is given by (3.10), the following points are direct consequences of the monotonicity properties of the reference solutions $\hat{U}$ and $\bar{U}$ recorded in Sect. 3.1:

- $\xi \mapsto f_+(\xi;U_r)$ is defined for $\xi \in [\xi_{\min},\infty)$ and decreases from $\sqrt{1+\beta}$ to 0+;
- $\xi \mapsto f_-(\xi;U_l)$ is defined for $\xi \in (-\infty,\xi_{\max}]$ and decreases from 0− to $-\sqrt{1+\beta}$;
- for each $\bar{C} \in \mathbb{R}$, $\xi \mapsto \bar{f}(\xi;\bar{C})$ is defined for all $\xi \in \mathbb{R}$ and increases from $-(1+\beta)$ to $1+\beta$; and
- for each $\xi \in \mathbb{R}$, $\bar{C} \mapsto \bar{f}(\xi;\bar{C})$ is defined for all $\bar{C} \in \mathbb{R}$ and is a decreasing function.

Since $-1 < \beta < 0$, we have $1+\beta < \sqrt{1+\beta}$, and the existence of unique solutions to the two equations in (4.17) is a direct consequence. Finally, since $\bar{f}(\xi;\bar{C})$ vanishes at $\xi = \bar{C}$, the result follows. □

For later reference, we introduce $\bar{\xi}^*_+ = \bar{\xi}^*_+(U_r)$ and $\bar{\xi}^*_- = \bar{\xi}^*_-(U_l)$ as the unique values for which

$$f_+(\bar{\xi}^*_+;U_r) = 1+\beta \qquad \text{and} \qquad f_-(\bar{\xi}^*_-;U_l) = -(1+\beta), \tag{4.18}$$

respectively. It follows from the proof of Lemma 4.1 that the range of $\bar{C} \mapsto \bar{\xi}_+(\bar{C})$ is $(\bar{\xi}^*_+,\infty)$, and that the range of $\bar{C} \mapsto \bar{\xi}_-(\bar{C})$ is $(-\infty,\bar{\xi}^*_-)$.

Next, consider the remaining Rankine–Hugoniot relations in (4.11) and (4.13). With the notation introduced above, these take the forms

$$\bar{K}_+(\cosh[|\alpha|\bar{U}(\bar{\xi}_+ - \bar{C})])^{-\beta} = K_+(1+\beta)|\sinh[|\alpha|\hat{U}(\bar{\xi}_+ - U_r)]|^{-\beta}\coth^2[|\alpha|\hat{U}(\bar{\xi}_+ - U_r)] \tag{4.19}$$

and

$$\bar{K}_-(\cosh[|\alpha|\bar{U}(\bar{\xi}_- - \bar{C})])^{-\beta} = K_-(1+\beta)|\sinh[|\alpha|\check{U}(\bar{\xi}_- - U_l)]|^{-\beta}\coth^2[|\alpha|\check{U}(\bar{\xi}_- - U_l)], \tag{4.20}$$

respectively, where we have written $\bar{K}_+$ for $\bar{K}$ in (4.11) and $\bar{K}_-$ for $\bar{K}$ in (4.13). According to Lemma 4.1, Eqs. (4.19) and (4.20) define $\bar{K}_\pm$ as functions of $\bar{C}$, and the goal is to argue that there is a unique value of $\bar{C}$ for which $\bar{K}_+(\bar{C}) = \bar{K}_-(\bar{C})$.

First, consider (4.19) and use the relations $|\sinh s| = |\tanh s|(1-\tanh^2 s)^{-\frac{1}{2}}$ and $\cosh s = (1-\tanh^2 s)^{-\frac{1}{2}}$ to obtain

$$\begin{aligned}\bar{K}_+(1-\tanh^2[|\alpha|\bar{U}(\bar{\xi}_+ - \bar{C})])^{\frac{\beta}{2}} \\ = K_+(1+\beta)|\tanh[|\alpha|\hat{U}(\bar{\xi}_+ - U_r)]|^{-\beta-2}(1-\tanh^2[|\alpha|\hat{U}(\bar{\xi}_+ - U_r)])^{\frac{\beta}{2}}.\end{aligned}$$

Using (4.15) to express $\tanh[|\alpha|\bar{U}(\bar{\xi}_+ - \bar{C})]$ in terms of $\tanh[|\alpha|\hat{U}(\bar{\xi}_+ - U_r)]$ and solving for $\bar{K}_+$ give

$$\bar{K}_+ = K_+F(X) \tag{4.21}$$

where

$$X = \tanh^2[|\alpha|\hat{U}(\bar{\xi}_+ - U_r)] \qquad \text{and} \qquad F(X) = (1+\beta)^{1+\beta}X^{-(\frac{\beta}{2}+1)}\left[\frac{1-X}{(1+\beta)^2 - X}\right]^{\frac{\beta}{2}}. \tag{4.22}$$

A calculation shows that $F(X)$ is a strictly decreasing function of $X \in (0,(1+\beta)^2)$ (which is the relevant range of $X$-values according to (4.15)), and that

$$F(X) \uparrow \infty \quad \text{as } X \downarrow 0, \text{ and } \quad F(X) \downarrow 0 \quad \text{as } X \uparrow (1+\beta)^2. \tag{4.23}$$

A similar argument using (4.20) and (4.16) shows that

$$\bar{K}_- = K_-F(Y) \tag{4.24}$$

where

$$Y = \tanh^2[|\alpha|\check{U}(\bar{\xi}_- - U_l)].$$

Introducing the strictly decreasing function

$$h(z) := \tanh^2[|\alpha|\hat{U}(z)],$$

so that $X \equiv h(\bar{\xi}_+ - U_r)$, and defining the function

$$G := F \circ h, \tag{4.25}$$

we rewrite (4.24) as

$$\bar{K}_+ = K_+ G(\bar{\xi}_+ - U_r). \tag{4.26}$$

Finally, recalling (4.14) which gives $Y \equiv h(U_l - \bar{\xi}_-)$, we rewrite (4.24) as

$$\bar{K}_- = K_- G(U_l - \bar{\xi}_-). \tag{4.27}$$

According to Lemma 4.1, the solutions $\bar{\xi}_\pm(\bar{C})$ of (4.15) and (4.16) are functions of $\bar{C}$. Using this together with (4.27)–(4.27), we define the functions

$$\bar{K}_+(\bar{C}) := K_+ G(\bar{\xi}_+(\bar{C}) - U_r) \qquad \text{and} \qquad \bar{K}_-(\bar{C}) := K_- G(U_l - \bar{\xi}_-(\bar{C})). \tag{4.28}$$

**Lemma 4.2.** *The functions $\bar{K}_\pm$ satisfy:*

- *$\bar{K}_+(\bar{C})$ is a strictly increasing function with range $(0,\infty)$ as $\bar{C}$ ranges over $\mathbb{R}$.*
- *$\bar{K}_-(\bar{C})$ is a strictly decreasing function with range $(0,\infty)$ as $\bar{C}$ ranges over $\mathbb{R}$.*

*It follows that there is a unique value of $\bar{C}$ such that $\bar{K}_+(\bar{C}) = \bar{K}_-(\bar{C})$.*

*Proof.* According to Lemma 4.1, both of $\bar{\xi}_\pm(\bar{C})$ are increasing functions of $\bar{C}$. More precisely, as $\bar{C}$ increases from $-\infty$ to $+\infty$, $\bar{\xi}_+(\bar{C})$ increases from the lower value $\bar{\xi}_+^*$ and up to $+\infty$, while $\bar{\xi}_-(\bar{C})$ increases from $-\infty$ and up to the upper value $\bar{\xi}_-^*$ (see (4.18)).

Now consider $\bar{K}_+(\bar{C})$ and recall the properties of the function $f_+(\xi; U_r)$ introduced in the proof of Lemma 4.1. It follows from what was just stated about the function $\bar{\xi}_+(\bar{C})$ that $f_+(\bar{\xi}_+(\bar{C}); U_r)$ decreases from $1+\beta$ to 0 as $\bar{C}$ increases from $-\infty$ to $+\infty$, and therefore $h(\bar{\xi}_+(\bar{C}) - U_r) = f_+(\bar{\xi}_+(\bar{C}); U_r)^2$ decreases from $(1+\beta)^2$ to 0. In turn, (4.23), (4.25), and $(4.28)_1$ then give that $\bar{K}_+(\bar{C})$ increases from 0 to $+\infty$ as $\bar{C}$ increases from $-\infty$ to $+\infty$.

Finally, consider $\bar{K}_-(\bar{C})$. Again, from the proof of Lemma 4.1 we have that $f_-(\bar{\xi}_-(\bar{C}); U_l)$ decreases from 0 to $-(1+\beta)$ as $\bar{C}$ increases from $-\infty$ to $+\infty$. Therefore, $h(U_l - \bar{\xi}_-(\bar{C})) = f_-(\bar{\xi}_-(\bar{C}); U_l)^2$ increases from 0 to $(1+\beta)^2$. It then follows from (4.23), (4.25), and $(4.28)_2$ that $\bar{K}_-(\bar{C})$ decreases from $+\infty$ to 0 as $\bar{C}$ increases from $-\infty$ to $+\infty$. □

Letting $\bar{C}$ be the unique value determined by Lemma 4.2, we make the definitions

$$\bar{K} := \bar{K}_+(\bar{C}) = \bar{K}_-(\bar{C}), \qquad \bar{\xi}_- := \bar{\xi}_-(\bar{C}), \qquad \bar{\xi}_+ := \bar{\xi}_+(\bar{C}).$$

The analysis above shows that with this choice the four parameters $\bar{C}$, $\bar{K}$, and $\bar{\xi}_\pm$, all of the Rankine–Hugoniot conditions (4.10)–(4.13) are satisfied. Finally, it follows from Lemma 4.1 that $\bar{\xi}_-$ and $\bar{\xi}_+$ are distinct numbers, showing that the solution of the GRP necessarily contain *exactly* two shock waves. This completes the proof of Theorem 1.1 for the case $\beta \in (-1, 0)$.

## 5. Self-similar GRPs for $\beta \in (0, \infty)$

In this section, we consider self-similar GRPs for the isothermal Euler system (1.2)–(1.3) with initial data (1.5) when $\beta > 0$. The analysis is quite similar to the case $\beta \in (-1, 0)$ and we therefore omit the details.

For $\beta > 0$, the Type I and Type II reference solutions $\hat{U}$, $\bar{U}$ were given in Sect. 3.2. The difference with the case $\beta \in (-1, 0)$ is that $\beta$, and hence also $\alpha$, now are positive (cf. (3.5)). This causes qualitative changes in the functions $\hat{U}$, $\bar{U}$, as reflected in Fig. 2. In particular, the solution $\hat{U}(\xi)$ is now increasing and defined for all $\xi \in \mathbb{R}$, while the solution $\bar{U}(\xi)$ is decreasing and only defined for $\xi \in [-\xi^*, \xi^*]$, with $\xi^*$ is given by (3.12).

The analysis in Sect. 4.1, which shows how the initial data determine the self-similar solution for large values of $|\xi| = \frac{|x|}{t}$, applies verbatim. The same holds for the calculations in Sect. 4.2 up to and including the statement of Lemma 4.1. The only difference is that the unique roots $\bar{\xi}_\pm(\bar{C})$ are both located within the interval $(\bar{C} - \xi^*, \bar{C} + \xi^*)$. The rest of the analysis in Sect. 4.2 applies to the case $\beta > 0$ with only minor changes in the arguments. In particular, the statement of Lemma 4.2 remains valid as stated. This completes the argument for the case $\beta > 0$ and thus the proof of Theorem 1.1.

## 6. Further properties

We include two results that describe the behavior of the solution along particle trajectories within the central region $\bar{\xi}_- t < x < \bar{\xi}_+ t$.

**Proposition 6.1.** *Assume $\beta \in (-1, \infty) \setminus \{0\}$ and let $(\rho(t,x), u(t,x))$ be the solution of a self-similar GRP for the isothermal Euler system (1.2)–(1.3) given by Theorem 1.1. Consider any particle trajectory $x(t)$ located within the central wedge $\bar{\xi}_- < \frac{x}{t} < \bar{\xi}_+$. Then, the density decreases (increases) along $x(t)$ when $-1 < \beta < 0$ ($\beta > 0$).*

*Proof.* Let $x(t)$ denote any particle trajectory within the central region, and let $U_0$ and $\Omega_0$ be the solutions of the similarity ODEs (2.6)—(2.7) that give the self-similar solution there. Using these ODEs, we obtain (with $\xi \equiv \xi(t) = \frac{x(t)}{t}$)

$$\begin{aligned} \frac{d}{dt}\rho(t, x(t)) &= \frac{d}{dt}[t^\beta \Omega_0(\xi)] = t^{\beta-1}\Omega_0(\xi)[\beta + \tfrac{\Omega_0'(\xi)}{\Omega_0(\xi)}(U_0(\xi) - \xi)] \\ &= -a^2 \beta t^{\beta-1} \frac{\Omega_0(\xi)}{(U_0(\xi) - \xi)^2 - a^2}. \end{aligned}$$

Recalling from Sects. 4 and 5 that the graph of the Type II solution $U_0(\xi)$ by construction is located within the 45°-strip $\{(\xi, U) \,|\, |U - \xi| < a\}$, while $\Omega_0$ is strictly positive, the claims follow. □

**Proposition 6.2.** *With the same assumption as in Proposition 6.1, we have that each particle trajectory $x(t)$ in the central wedge satisfies*

$$\lim_{t \uparrow \infty} \dot{x}(t) = \bar{C},$$

*where $\bar{C}$ is given by Lemma 4.2*

*Proof.* Since the two straight lines $x = \bar{\xi}_- t$ and $x = \bar{\xi}_+ t$ are admissible 1- and 2-shocks, respectively, it follows that particle trajectories cross into the central wedge as time increases. We have

$$\dot{x}(t) = u(t, x(t)) = U_0(\xi(t)),$$

where $\xi(t) = \frac{x(t)}{t}$. Since $U_0$ is continuous and satisfies $U_0(\bar{C}) = \bar{C}$ by construction, it suffices to verify that

$$\lim_{t \uparrow \infty} \xi(t) = \bar{C}. \tag{6.1}$$

For concreteness, consider a trajectory $x(t)$ that enters through the left edge $x = \bar{\xi}_- t$ at some time $t_0 > 0$ and consider the case $\beta > 0$. For $t \geq t_0$, we have

$$\dot{\xi}(t) = \frac{1}{t}(U_0(\xi(t)) - \xi(t)), \tag{6.2}$$

which is nonnegative since the point $(\xi(t), U_0(\xi(t)))$ in this case lies within the 45°-strip $\{(\xi, U) \,|\, 0 < U - \xi < a\}$. Thus $\xi(t)$ increases with time. Assume for contradiction that (6.1) fails; there is then an $\epsilon > 0$ such that

$$\xi(t) \leq \bar{C} - \epsilon \qquad \text{for all } t \geq t_0. \tag{6.3}$$

As $U_0(\xi)$ is strictly decreasing in the case under consideration, we get that there is a $\delta > 0$ so that

$$U_0(\xi(t)) \geq \bar{C} + \delta \qquad \text{for all } t \geq t_0. \tag{6.4}$$

Recalling that $U_0$ is a 45°-translate of the reference Type II solution, we obtain from (3.4), (6.2), and (6.4) that

$$\dot{\xi}(t) = \frac{\mu}{t}\tanh[\alpha(U_0(\xi(t)) - \bar{C})] \geq \frac{\mu}{t}\tanh[\alpha\delta] \qquad \text{for all } t \geq t_0.$$

Since $\mu$, $\alpha$, and $\delta$ are all strictly positive numbers, integrating the last inequality from $t = t_0$ to $t = \infty$ yields a contradiction. The other cases are proved by a similar argument. □

## Acknowledgements

This work was supported in part by NSF award DMS-1813283. The authors gratefully acknowledge the suggestions of the anonymous referee which helped to improve the presentation.



## References

[1] Chen, G., Pan, R., Zhu, S.: Singularity formation for the compressible Euler equations. SIAM J. Math. Anal. **49**(4), 2591–2614 (2017). https://doi.org/10.1137/16M1062818

[2] Chen, G.: Optimal time-dependent lower bound on density for classical solutions of 1-D compressible Euler equations. Indiana Univ. Math. J. **66**(3), 725–740 (2017). https://doi.org/10.1512/iumj.2017.66.5988

[3] Chen, G.: Optimal density lower bound on nonisentropic gas dynamics. J. Differ. Equ. **268**(7), 4017–4028 (2020). https://doi.org/10.1016/j.jde.2019.10.017

[4] Dafermos, C.M.: Hyperbolic Conservation Laws in Continuum Physics, 4th edn. Grundlehren der Mathematischen Wissenschaften [Fundamental Principles of Mathematical Sciences], vol. 325. Springer, Berlin (2016)

[5] DiPerna, R.J.: Convergence of the viscosity method for isentropic gas dynamics. Commun. Math. Phys. **91**(1), 1–30 (1983)

[6] Glimm, J.: Solutions in the large for nonlinear hyperbolic systems of equations. Commun. Pure Appl. Math. **18**, 697–715 (1965). https://doi.org/10.1002/cpa.3160180408

[7] Greenspan, H.P., Butler, D.S.: On the expansion of a gas into vacuum. J. Fluid Mech. **13**, 101–119 (1962). https://doi.org/10.1017/S0022112062000543

[8] Jang, J., Masmoudi, N.: Vacuum in gas and fluid dynamics. Nonlinear conservation laws and applications, IMA Vol. Math. Appl., vol. 153. Springer, New York, pp. 315–329 (2011)

[9] Lax, P.D.: Hyperbolic systems of conservation laws. II. Commun. Pure Appl. Math. **10**, 537–566 (1957). https://doi.org/10.1002/cpa.3160100406

[10] Lax, P.D.: Development of singularities of solutions of nonlinear hyperbolic partial differential equations. J. Math. Phys. **5**, 611–613 (1964). https://doi.org/10.1063/1.1704154

[11] LeFloch, P.G., Shelukhin, V.: Symmetries and global solvability of the isothermal gas dynamics equations. Arch. Ration. Mech. Anal. **175**(3), 389–430 (2005). https://doi.org/10.1007/s00205-004-0344-3

[12] LeFloch, P.G., Yamazaki, M.: Entropy solutions of the Euler equations for isothermal relativistic fluids. Int. J. Dyn. Syst. Differ. Equ. **1**(1), 20–37 (2007). https://doi.org/10.1504/IJDSDE.2007.013742
[13] Nishida, T.: Global solution for an initial boundary value problem of a quasilinear hyperbolic system. Proc. Jpn. Acad. **44**, 642–646 (1968)
[14] Riemann, B.: Collected Papers. Kendrick Press, Heber City (2004). Translated from the 1892 German edition by Roger Baker, Charles Christenson and Henry Orde
[15] Smoller, J.: Shock Waves and Reaction–Diffusion Equations, 2nd edn, Grundlehren der Mathematischen Wissenschaften [Fundamental Principles of Mathematical Sciences], vol. 258. Springer, New York (1994)

Helge Kristian Jenssen and Yushuang Luo
Department of Mathematics
Penn State University
University Park, State College PA16802
USA
e-mail: jenssen@math.psu.edu

Yushuang Luo
e-mail: yzl55@psu.edu

(Received: September 24, 2020; revised: February 16, 2021; accepted: February 23, 2021)